A CCR4 antagonist reverses the tumor-promoting microenvironment of renal cancer.

Berlato, C; Khan, MN; Schioppa, T; Thompson, R; Maniati, E; Montfort, A; Jangani, M; Canosa, M; Kulbe, H; Hagemann, UB; Duncan, AR; Fletcher, L; Wilkinson, RW; Powles, T; Quezada, SA; Balkwill, FR

A CCR4 antagonist reverses the tumor-promoting microenvironment of renal cancer

Chiara Berlato[1], Moddasar N. Khan[1], Tiziana Schioppa[1,2], Richard Thompson[1], Eleni Maniati[1], Anne Montfort[1], Maryam Jangani[1], Monica Canosa[1], Hagen Kulbe[1,3], Urs B Hagemann[4], Alexander Duncan[4], Laura Fletcher[5], Robert W. Wilkinson[6], Thomas Powles[1], Sergio A. Quezada[7], Frances Balkwill[1,8]

[1] Barts Cancer Institute

Queen Mary University of London

Charterhouse Square

London EC1M 6BQ, UK

[2] Department of Molecular and Translational Medicine,

University of Brescia,

Brescia, Italy

[3] Department of Gynecology,

Charité Universitätsmedizin

Berlin, Germany

[4] Affitech Research AS

Oslo Research Park

Gaustadalléen 21 N-0349 Oslo, Norway

[5] Cancer Research Technology Ltd

Angel Building

407 St John Street, London EC1V 4AD, UK

[6] MedImmune Ltd, Granta Park,

Cambridge, CB21 6GH, UK

[7] Cancer Immunology Unit,

Research Department of Haematology,

UCL Cancer Institute,

University College London, UK

Huntley St, London WC1E 6DD, UK

[8] Senior and corresponding author

Frances R Balkwill

Barts Cancer Institute

Queen Mary University of London

Charterhouse Square

London EC1M 6BQ, UK

Tel: + 442078823576

f.balkwill@qmul.ac.uk

Conflict of interest: Affitech AS funded some of the research in this paper.

Abstract

The chemokine receptor CCR4 was highly expressed in human renal cell carcinoma (RCC) biopsies and there were abnormal levels of CCR4 ligands in RCC patient plasma. An anti-CCR4 antagonistic antibody had novel anti-tumor activity in the mouse RCC RENCA model. Inhibition of CCR4 did not reduce the proportion of infiltrating leukocytes in the tumor microenvironment but altered the phenotype of myeloid cells, increased NK cells and Th1 cytokine levels, as well as reducing the immature myeloid cell infiltrate, and blood chemokine levels. Although prominent changes were seen in the myeloid compartment, the anti-CCR4 antibody had no effects on RENCA tumors grown in T-cell deficient mice, and anti-tumor activity was abrogated by treatment with an anti-Class II MHC antibody. We conclude the action of the anti-CCR4 antibody required the adaptive immune system and was dependent on CD4+ T cells. Moreover, when Th1-polarised normal CD4+ T cells were exposed to the CCR4 ligand CCL17 production of IFNγ was reduced suggesting that CCR4 may be more widely involved in Th1/Th2 regulation. The anti-CCR4 antibody, alone, or in combination with other immune modulators, may be of interest in human solid cancers with high levels of CCR4-expressing tumor-infiltrating leukocytes and abnormal plasma CCR4 ligand levels.

Introduction

Tumor microenvironments possess complex chemokine networks that contribute to the extent and phenotype of the host infiltrate (1-3). In addition, malignant cells may gain functional chemokine receptors, often as a consequence of oncogenic mutations, allowing them to respond to distant chemokine gradients during metastatic spread (4, 5).

The chemokine receptor CCR4 is expressed on circulating and tissue-resident T cells, being predominantly associated with a Th2 phenotype (6-8) as well as on other T helper cells (9). CCR4 is also highly expressed on circulating Tregulatory cells, Tregs, and on Tregs recruited at tumor sites in ovarian cancer (10) and in glioblastoma (11). In ovarian cancer, CCL22 is found both in the tumor tissue and in macrophages isolated from ascitic fluid (9). In hepatocellular carcinoma, malignant cell-produced CCL22 recruited CCR4+ Tregs that facilitated immune escape of malignant cells (12). Similarly, in breast cancer, CCR4+ Tregs, recruited by CCL22 in the tumor microenvironment, are predictive for a worse prognosis (13). A second breast cancer study found reduced overall survival and high CCR4 expression in tumor biopsies (14). Finally, in a cohort of 753 patients with gastric adenocarcinoma, positive staining for CCR4 was also associated with a poorer prognosis (15).

CCR4 also plays a role in haematological malignancies and there are now clinical trials of an anti-CCR4 antibody, mogamulizumab, which has enhanced ADCC (antibody-dependent cell-mediated cytotoxicity) activity. Mogamulizumab is approved in Japan for the treatment of relapsed Adult T cell leukemia (ATL)(16) and has also been tested in

patients with relapsed peripheral-T cell lymphoma (PTLC), and cutaneous T-cell lymphoma (CTLC) (17). The treatment is indicated for patients with CCR4-positive leukemia cells, but might also act by reducing the number of Tregs in cancer patients (18).

In this paper we have investigated CCR4 as a target in renal cell carcinoma, RCC, using patient samples and an orthotopic mouse RCC model. We have found abnormal levels of CCR4 and its ligands in human RCC biopsies and plasma samples. In pre-clinical experiments we found that Affi-5, a fully human anti-CCR4 antibody with antagonistic activity, described in (19), has a novel anti-tumor activity in a renal cancer model. Inhibition of CCR4 did not reduce the proportion of CCR4-positive infiltrating leukocytes in the tumor microenvironment but altered the phenotype of the immune infiltrate, affecting in particular the phenotype of myeloid cells, and increasing the number of infiltrating NK cells. These effects were dependent on the adaptive immune system and required functioning CD4+ T cells. The antibody also altered the phenotype of tumor-associated macrophages in the B16 melanoma model. Inhibition of CCR4, alone, or in combination with other immune modulators, may be a valuable therapeutic approach in human cancers with high levels of CCR4 in the tumor microenvironment and abnormal plasma CCR4 ligand levels.

Results

CCR4 and its ligands in human renal cell carcinoma

This study was initially prompted by finding abundant CCR4 mRNA in biopsies from renal cancers as compared to normal kidney (Figure 1A). CCR4 protein was also detected by immunohistochemistry, IHC, on malignant cells and leukocytes in a tissue microarray, TMA, constructed from 57 advanced renal cell carcinoma, RCC, patient biopsies (Figure 1B, Supplementary Figure 1A). Of the 173 cores in the TMA, 157 showed positive CCR4 staining. 75% of the biopsies were classified as clear cell with others classified as papillary RCC. There was a significant positive correlation between CCR4 positivity and the extensive T cell (CD3+) or macrophage (CD68+) infiltrates in the tumor cores (Supplementary Figure 1B-D), suggesting that CCR4 may be important in the trafficking of tumor-associated leukocytes.

The CCR4 ligands CCL22 (MDC) and CCL17 (TARC) were also expressed in the RCC tumors (Figure 1B, Supplementary Figure 1A). CCR4 was weakly expressed in normal kidney but the ligands could be detected in normal kidney tubules (Supplementary Figure 1A).

We next compared plasma concentrations of CCL17 and CCL22 from patients with advanced RCC with age-matched controls using the MesoScale Discovery electrochemiluminescence system. The concentration of CCL17 in plasma was significantly higher in patients; however, the concentration of CCL22 was significantly lower in the patients compared to controls (Figure 1C, D). The CCL17: CCL22 ratio was also significantly different between the two groups and four-fold higher in patients compared to controls (Figure 1E). Moreover, a high CCL17: CCL22 ratio correlated with

lower progression-free and overall survival rates (Figure 1F, G) but this association was not seen if the individual chemokines were examined (Supplementary Figure 1E, F) suggesting that activity of both chemokines is important in RCC biology. In our cohort, CCR4 expression, as determined by IHC on the TMAs, was not predictive of clinical outcome (not shown).

Renal cancer cell lines have functional CCR4 receptors

As we had detected CCR4 and its ligands in malignant cells in tumor biopsies, we next studied RCC cancer cell lines. RCC cell lines 786-O and A498 (human) and RENCA (murine) expressed cell surface CCR4 as determined by flow cytometry. The human cell lines had detectable intracellular CCL17 and CCL22 (Supplementary Figure 2) and these chemokines were also present in the tissue culture medium during three days incubation (CCL17 300 pg/10^6 cells, CCL22 2 ng/10^6 cells). RENCA cells also secreted CCL17 (200 pg/10^6 cells) and CCL22 (10 pg/10^6 cells) in the medium during three days incubation.

Both CCR4 ligands stimulated migration of the human cell line 786-O (Supplementary Figure 3A, B). Similar data were obtained for A498 (data not shown) and murine RENCA cells (Supplementary Figure 3A, B) with characteristic bell-shaped concentration-response curves typical of chemokine-mediated migration, implicating that the receptor can be functional on malignant cells. shRNA to CCR4 abolished CCR4 staining in the RCC cells as well as their migration to CCL17 (Supplementary Figure 3C, D). In addition, a fully human anti-CCR4 antagonistic antibody, Affi-5 (19), abrogated the migration of 786-O

cells to CCL17, further confirming that the CCR4 receptor is functional in the tumor cells (Supplementary Figure 3E).

Anti-tumor activity of an anti-CCR4 antibody

Taken together, the above data and the published literature suggest that CCR4 is a therapeutic target of interest in human solid cancers, especially as it is expressed by both malignant cells and tumor-infiltrating leukocytes. We therefore conducted pre-clinical experiments using the Affi-5 antagonistic antibody to CCR4 in the RENCA mouse RCC model. Affi-5 inhibited migration of RENCA cells to murine CCL17 and CCL22 showing that the antibody was antagonistic to murine CCR4 as well as human CCR4 (Figure 2A, Supplementary Figure 3F). Affi-5 did not influence the growth or viability of either human or murine RCC cells in normal or low serum or their release of CCR4 ligands (data not shown).

RENCA cells labelled with luciferase were grown orthotopically in their syngeneic hosts, wild-type Balb/c mice, by injection into the renal capsule of the left kidney. Mice reached humane endpoint during the course of tumor growth between 17-21 days post implantation. Anti-CCR4 antibody treatment significantly inhibited tumor burden as measured by tumor weight and bioluminescence as compared to treatment with an isotype control antibody (Figure 2B,C). Figure 2B shows the mean tumor weights at end point from six independent experiments with 20 mg/kg Affi-5 versus an isotype control, while Figure 2C shows a typical experiment using bioluminescence as a measure of tumor growth. 10 mg/kg Affi-5 also had significant anti-tumor activity ($p=0.0003$) (six

experiments, C n=39, T n=42, p=0.0003, Figure 2D). There was a significant reduction in the serum concentration of the CCR4 ligand CCL17 in treated mice (Figure 2E). In contrast, serum concentration of CCL22 was low and did not change following treatment (Figure 2F). Analysis of CCL17 and CCL22 expression in tumor lysates showed that, adjusted for tumor size, CCL17 levels are stable while CCL22 levels are higher in anti-CCR4 treated tumors (not shown), suggesting that the decrease in CCL17 circulating levels might reflect a reduction in tumor size.

Actions of the anti-CCR4 antibody on tumor-associated macrophages

We considered that from the data presented previously, as well as from the published literature, the mechanism of anti-CCR4 inhibition on tumor growth could involve direct effects on malignant cells and/or on leukocytes. To investigate mechanisms of action of the anti-CCR4 antibody, we studied single cell suspensions from the treated tumors. Several cell types were positive for CCR4 staining in control tumors: macrophages (CD45+ F4/80+ CD11b+) and different T cell subtypes, such as CD4+ (CD45+ CD3+ CD4+ FoxP3-), CD8+ lymphocytes (CD45+ CD3+ CD8+) and Tregs (CD45+ CD3+ CD4+ FoxP3+) (Supplementary Figure 4). NK cells were also weakly positive for CCR4 staining (Supplementary Figure 4). Compared to the leukocyte populations, CD45- cells, which contain the malignant cell population, were only weakly positive for CCR4 (Supplementary Figure 4).

As tumor associated macrophages (TAMs) showed expression of CCR4, we first studied the numbers and phenotype of these cells. The number of TAMs (gated as CD45+ CD11+

CD11b+ F4/80+) per mg of tumor did not differ significantly between Affi-5-treated and control-treated tumors (Figure 3A). However, the phenotype of the macrophages was affected by treatment. TAMs from Affi-5 treated mice expressed significantly higher levels of MHCII and lower levels of mannose receptor (MR) compared to TAMs from control-treated mice (Figure 3B, C). In the spectrum of phenotype of macrophage activation, low MHCII expression and high MR levels are associated with an 'M2' phenotype, which promotes tissue repair and cell proliferation (20). Conversely, high MHCII expression and low MR expression are characteristic of an 'M1' macrophage phenotype, associated with anti-tumor activity. To further characterise the TAM phenotype, we extracted mRNA from macrophages from Affi-5 and control-treated tumors and analysed them for arginase and inducible nitric oxide synthase (NOS2) expression. The arginase: NOS2 expression ratio was significantly lowered by anti-CCR4 treatment (Figure 3D). Purified Affi-5 treated macrophages also showed increased intracellular TNF, further evidence for an 'M1' cytotoxic phenotype (Figure 3E). Taken together, these data imply that the phenotype of macrophages from anti-CCR4 treated tumors was altered compared to isotype control-treated tumors and displayed several characteristics associated with an anti-tumor response.

We next asked if CCR4 inhibition could have similar activities in another mouse cancer model, testing Affi-5 in the B16 melanoma model. As shown in Supplementary Figure 5, treatment altered the tumor-associated macrophage phenotype with a significant increase in MHC Class II in myeloid cells in two separate experiments (Supplementary

Figure 5A). There was, however, no effect on MR expression (Supplementary Figure 5B) or tumor weight (Supplementary Figure 5C) in this rapidly growing model.

Actions of the anti-CCR4 antibody on T cells in the tumor microenvironment

We next examined changes among the CD3+ T cells, which were also positive for CCR4 in the RENCA tumor microenvironment. The number of CD3+ cells per mg of tumor was significantly higher in Affi-5-treated tumors compared to controls (Figure 4A). As CCR4 has been implicated in the recruitment of Tregs at tumor sites (12, 13), we hypothesised that treatment with anti-CCR4 would reduce the number of CCR4+ Tregs, as observed in adult T-cell leukemia patients treated with mogamulizimab (18). However, the number of Tregs per mg of tumor was higher in anti-CCR4 treated tumors (Figure 4B). Also the number of CD4 effector cells and CD8 cells per mg of tumor was increased with treatment (Figure 4B). As a result of these changes, the ratios of CD4 T effector or CD8 T cells to Tregs in tumors were unaffected by Affi-5-treatment (Figure 4C).

However, there was an increase in the amount of Th1 cytokines compared to Th2 cytokines in the Affi-5-treated tumor lysates (Figure 4D), which could help explain the M2/M1 switch observed in the TAMs.

We next explored in more detail the phenotype of CD4 effector and CD8 cells. The number of CD4 cells positive for IFNγ expression was increased in treated tumors (Figure 4E), while it was unaltered for the CD8 cells (Figure 4F). Moreover, CD8 staining for granzyme B was not significantly altered by treatment (Figure 4G). Collectively, these data suggested a role for CD4 cells in the anti-tumor activity of the anti-CCR4 antibody.

Other treatment-induced changes to tumor-infiltrating leukocyte populations

We observed repeatedly a significant increase in tumor NK cells as a proportion of total CD45+ cells (Figure 5A), while the proportion of granzyme B-positive NK cells was not altered (not shown). The effects on NK cells was due to changes in cell number, as a significant increase in terms of NK cells/mg tumor could be observed ($p=0.03$) (Figure 5B). Also myeloid derived suppressor cells (MDSCs), characterised as CD45+ CD11b+ Gr1+, constituted a reduced percentage of the CD45+ infiltrate in tumors from treated mice compared to control-treated (Figure 5C), as there were less granulocytic ($Gr1^{high}$) and monocytic ($Gr1^{int}$) MDSCs in treated tumors. As for the MDSCs cells there was some variability between experiments in terms of numbers of cells so we have expressed the results as fold change of cells/mg of tumor. Pooling results from four experiments we see a significant reduction in treated tumors ($p=0.017$) (Figure 5D). A similar reduction of granulocytic ($Gr\text{-}1^{high}$) and monocytic ($Ly6C^{high}$) MDSCs was seen in the spleen of treated mice compared to control mice (Figure 5E). To determine whether the accumulated CD11b+ Gr1+ have a suppressive phenotype and could really be identified as MDSCs, we performed immunosuppression assays using T cells as effectors. Increasing amounts of MDSCs from the tumors of untreated mice effectively suppressed proliferation of activated CD4 and CD8 cells isolated from naïve splenocytes (Figure 5F). Similarly, splenic MDSCs isolated from tumor-bearing mice suppressed proliferation of CD4 and CD8 cells (not shown).

Further investigation of CCR4 receptor on tumor CD4+ T cells

As in our model we observed changes to cells of both the adaptive and innate immune response, and some of our evidence pointed to involvement of CD4+ T cells, we wanted to better understand the interplay between these different components. Affi-5 did not inhibit RENCA tumor growth in T-cell deficient nude mice (Figure 6A) and there was also no effect on macrophage phenotype or extent of NK cell infiltrate in tumors in nude mice (Figure 6B-D). This suggested that adaptive immunity, especially via CD4+ T cells, was upstream of the actions on the cells of the innate immune system.

To further investigate a role for CD4 T cells in the anti-tumor actions of Affi-5, we combined this agent with a neutralising antibody to MHC Class II. This completely abrogated the effects of the anti-CCR4 antibody on RENCA tumor weight (Fig 6E), macrophage MHC Class II (Figure 6F) and mannose receptor expression (Figure 6G) and percentage of NK cells in the tumor microenvironment (Figure 6H).

We concluded that CD4 T cells are essential mediators of the actions of the anti-CCR4 receptor antibody Affi-5, and were required for the observed changes in macrophage phenotype and proportion of NK cells.

CCR4 function in normal T cells

Our results led us to question whether CCR4 might be involved in direct regulation of Th1 and Th2 responses in normal CD4+ T cells. To explore this, we developed an *in vitro* assay in which CD4+ T cells were purified from splenocytes of healthy mice, and polarized to a Th1 response with IL-12 and IL-2 in the presence of anti-CD3 and anti-

CD28 beads. This treatment stimulated production of IFNγ over the course of three days. When CCL17 was added to the CD4+ cells one day after the initial stimulation, a significant reduction in the production of IFNγ was observed (Figure 7A). Although CCL22 produced a similar trend, it was markedly weaker than CCL17 in inhibiting Th1 polarization (Figure 7A). The action of CCL17 on CD4+ cells *in vitro* was abolished by addition of the anti-CCR4 antibody (Figure 7B, C). These results indicate that CCL17 might play a role in directly inhibiting the Th1 response, and provide more mechanistic insight into the action of Affi-5. CCL17 in the tumor microenvironment might be secreted by many cell types, among which M2 polarized macrophages (21). To support this hypothesis we measured mRNA levels for CCL17 and 22 in the different cell populations of the tumor microenvironment. Macrophages showed the highest expression of the two chemokines (Supplementary Figure 6), although a contribution from other cell types cannot be excluded.

Is antibody-dependent cell-mediated cytotoxicity, ADCC, involved in the anti-tumor action of the anti-CCR4 antibody?

Finally, as ADCC is implicated in the mechanisms of action of the anti-human CCR4 antibody currently used clinically in treatment of haematological malignancies (16), we investigated the role of ADCC in the actions of Affi-5. While it is possible that murine Fc receptors would interact with a human antibody (22), both a defucosylated (which was used in all the experiments presented up to this point) and fucosylated version of Affi-5 antibody had similar and significant anti-tumor effects (Figure 8A). Moreover, the CCR4

antagonist Affi-5 retained anti-tumor activity on RENCA cells in which CCR4 was silenced by shRNA (Figure 8B, C). This result indicates that the anti-tumor effect of Affi-5 occurs primarily through modulation of non-malignant cells in the tumor microenvironment. This is not entirely unexpected since *in vivo* CD45- cells, which would comprise the RENCA cells, expressed low levels of CCR4 (Supplementary Figure 4). However, as this antibody has a reported ADCC activity against human lymphoma cells (19), it may act by ADCC on other tumor cells where CCR4 expression is higher.

Levels of PD-L1 and CTLA4 after treatment

Immune checkpoint targeting has proven to be a promising approach in the treatment of RCC. Therefore we investigated whether the anti-CCR4 treatment had an impact on immune checkpoint ligands. As shown in Supplementary Figure 7, CTLA4 expression on Tregs, and PD-L1 expression on macrophages, CD3+ T cells and CD45- cells was retained after anti-CCR4 treatment. This would suggest that, as the anti-CCR4 treatment displays novel actions on different components of the immune infiltrate, it could be a good candidate to be administered together with promising immune checkpoint inhibitors.

Discussion

In this study, we provide a comprehensive analysis of the expression of the chemokine receptor CCR4 and its ligands CCL17 and CCL22 in a solid tumor. We present evidence that CCR4 is expressed at significant levels in renal cancer biopsies, where it is associated with the extent of immune infiltrate. Also CCL17 and CCL22 expression is altered in renal cancer tissue and in the plasma of patients. In fact, a high CCL17:CCL22 ratio in plasma is associated with a worse prognosis. This is reminiscent to what observed in other solid tumors, where there is high CCR4 expression that is generally associated with a poor prognosis (14) (15). CCL22 is also detected in the tumor microenvironment of ovarian, hepatocellular and breast cancer (10) (12, 13). Our work is further supported by a recent multivariate analysis of CCR4 expression in 53 RCC patient biopsies where CCR4 expression was an independent risk factor for poor prognosis and overall survival (23). Taken together, these observations suggest that CCR4 is an attractive therapeutic target in solid cancers.

In the current work, we have not considered a role for the chemokines, CCL2 and CCL5, that may also bind to CCR4 as CCL17 and 22 have the highest affinity for the receptor but in future studies it would be interesting to assess the effect of CCR4 inhibitions on their local and systemic levels.

In this study we report for the first time that an anti-CCR4 antibody has activity in a solid cancer model. As CCR4 is expressed on a number of different immune cells, we had expected that the CCR4 antibody would reduce the number of tumor-infiltrating leukocytes as part of its mechanism of action, but this did not occur. In particular, we

did not observe an effect on the number of infiltrating Tregs, which are thought to be recruited though CCR4 in the tumor microenvironment of different tumor types (11) (13) (12). In fact the antibody caused unexpected changes in the phenotype of myeloid cells in the RENCA tumor microenvironment from potentially pro- to anti-tumor. Tumor associated macrophages mainly consist of a population with little cytotoxicity for tumor cells because of their limited production of NO and proinflammatory cytokines. At the same time, TAMs also possess poor antigen-presenting capability (20). This has led to the notion that depleting TAMs from the tumor microenvironment is an interesting target in cancer therapy. However, it was shown recently that inhibition of the macrophage cell surface receptor CSF1R with a small molecule inhibitor in a model of glioblastoma was able to reduce tumor progression by reducing the M2 polarization of TAMs (24). This work proved that modification of TAM tumor-promoting functions may have a significant impact on tumor growth and that depletion is not strictly necessary for an effective TAM-targeted therapy. In our work, the use of an anti-CCR4 antibody achieves, through a different mechanism of action, a similar change of TAM phenotype, which results in a reduction of tumor growth. There is an interesting human correlate in renal cancer to our experimental data, suggesting that stimulating an M2/Th2 to M1/Th1 response may be of therapeutic value. In a recent analysis of the intra-tumoral immunologic profile of RCC biopsies, M2 macrophage markers correlated with a poor prognosis and tumor iNOS mRNA levels with a good prognosis (25). To confirm the importance of macrophages in the mechanism of action of Affi-5, a depletion experiment with clodronate liposomes was set up, but the partial depletion of the

macrophages was accompanied by an M1 polarization of the remaining macrophages (not shown), thus invalidating this model for testing our hypothesis. The potential of the anti-CCR4 antibody was also suggested in the B16 melanoma experiments where we found an increase in Class II MHC expression. However, this 'partial switch' was not enough to generate an anti-tumor effect.

As part of the multiple effects of the anti-CCR4 antibody, we also observed a significant increase in NK cells, as well as reduction in MDSCs and circulating CCL17, which can additionally contribute to decreased tumor growth. To determine the contribution of these different populations infiltrating the tumors, we have extensively attempted to deplete NK cells and MDSCs in this model. However, while systemic depletion was successful, we never obtained a satisfactory depletion in the tumor microenvironment. As proven by the experiment in nude mice, these multiple effects are not directly mediated by leukocytes of the innate immune system, but are dependent on the adaptive immune system. Moreover, disrupting the MHCII: TCR interaction abolished the therapeutic effect of the anti-CCR4 antibody and also impacted on innate immunity thus proving an essential role for CD4 cells, linked to their ability to secrete IFNγ. Our *in vitro* assay further supported the hypothesis that the CCR4: CCL17 axis may be involved in maintaining Th2 responses. To our knowledge, the effects described here of CCR4 inhibition in this tumor microenvironment are novel.

We had also predicted that the anti-CCR4 antibody Affi-5 may have ADCC activity in the RENCA model, especially on the malignant cells, but the RENCA cells *in vivo* had low expression of CCR4. CCR4 is strongly expressed in several human T-cell malignancies.

Mogamulizumab (KW-0761; POTELIGIO®), a humanised fucosylated anti-CCR4 antibody that markedly enhances ADCC, is used in the treatment of patients with relapsed or refractory CCR4-positive ATL in Japan (26). Recently it also received approval in Japan for relapsed or refractory CCR4-positive peripheral T-cell lymphoma (PTCL) and cutaneous T-cell lymphoma (CTCL). We could find no evidence that Affi-5 was working via ADCC in our model system but this does not preclude such an action in other models or patients where malignant cells have higher levels of CCR4. Neither, we would suggest, does it preclude Mogamulizumab having other actions in the tumor microenvironment. Neither could we find evidence that the anti-CCR4 antibody had direct effects on the CCR4 expressing malignant cells. This may be because the CD45- population, which contained the malignant cells, expressed low levels of CCR4 in the tumor microenvironment. In addition RENCA tumors growing in nude mice did not respond to the anti-CCR4 antibody. As anti-CCR4 inhibited RENCA cell migration *in vitro*, it is possible that the antibody had an anti-metastatic effect but it was not possible to measure this in our model system.

In summary, we have described here a new therapeutic strategy to target solid tumors with a significant CCR4 expression in the tumor microenvironment. As targeting CCR4 in haematological malignancies has shown manageable side effects, this approach could readily be translated into the clinic. Moreover, this opens the possibility for evaluation of combinations of CCR4 inhibition with other immune-modulatory agents. Inhibition of CCR4 had multiple actions in the RCC experimental tumor microenvironment – but predominantly there was evidence of a Th2/M2 to Th1/M1 switch. CCR4 inhibition also

increased Class II MHC expression on tumor-associated macrophages in the B16 model. As Tregs infiltration or CD8 activation were not affected and the antibody did not alter levels of CTLA4 and PD-L1 in the renal tumor microenvironment, there is a strong rationale for a combination with immune checkpoint blockade. Also combinations with anti-CD40 agonistic antibodies would be an attractive option, as stimulating macrophage activation in a Th1 skewed environment may increase a host anti-tumor response.

Methods

Reagents

Recombinant human chemokines CCL17 (300-30) and CCL22 (300-36) were purchased from Peprotech (Rocky Hill, NJ). Recombinant mouse CCL17 (529-TR) and CCL22 (439-MD) were purchased from R&D Systems (Minneapolis, MN).

RNA isolation and RT-PCR

RNA from sorted macrophages was extracted with the RNeasy Micro Kit (Quiagen, Hilden, Germany) and amplified with the Ovation PicoSL WTA System V2 (NuGen, San Carlos, CA). Real-time RT-PCR analysis was performed using TaqMan assays (Applied Biosystems, Foster City,CA): CCR4 (Hs99999919_m1), 18s (4310893E), ArginaseI (Mm00440502_m1), iNOS (Mm99999062_m1) with the ABI StepOnePlus instrument (Applied Biosystems).

Renal tissue and patient plasma samples

Patients samples were collected under the Ethical Number MREC 02/8/78. Patients had locally advanced or metastatic renal cell carcinoma (RCC), who had progressed after first-line cytokine-based therapy (for locally advanced disease) or, were intolerant to first line cytokine-based therapy (for locally advanced or metastatic disease). The TMA was mainly comprised of clear cell renal carcinomas (75%), with some biopsies classified as papillary renal cancer. Clear cell renal carcinomas were identified using standard immunohistochemistry and CAIX staining. CCR4 was detected on the malignant cells from 153 of 173 malignant tumors, clear cell and non-clear cell, in our TMA. Controls were age-matched individuals with no malignancies.

Immunohistochemistry

Paraffin-embedded sections (4 μm) were dewaxed and dehydrated and antigen retrieval was performed by microwaving sections in Antigen Unmasking Solution (Vector, H-3300) for 9 min. After blocking with the appropriate serum, samples were incubated overnight at 4°C using primary antibodies: CCR4 (ab1669 1:300; Abcam, Cambridge, UK), CCL17 (ab182793 1:100; Abcam), CCL22 (500-P107 1:20; Peprotech), CD3 (A0452, 1:100, Dako, Santa Clara, CA), CD68 (M0876 1:50, Dako). Following incubation with a biotinylated secondary antibody (anti-goat, anti-rabbit or anti-mouse IgG, 1:200, Vector Laboratories, Burlingame, CA) for 30 min at room temperature, antigens were revealed with 3,3'-diaminobenzidine (Sigma-Aldrich, St. Loius, MO). Omission of the primary antibody and isotype control antibody were used as negative controls. The scoring for intensity of staining on positive cells was as follows: 0 (no expression), 1 (low expression) and 2 (high expression).

ELISA and Mesoscale Discovery System

Human CCL17 and CCL22 were determined from plasma with Mesoscale Discovery System plates (K151BGC-1 Human TARC Ultra-Sensitive Kit and Human MDC Ultra-Sensitive Kit, K151BAC, Mesoscale Diagnostic, Rockville, MD). Mouse CCL17 and CCL22 were determined from plasma or serum with Mouse CCL17/TARC Quantikine ELISA Kit (MCC170) or Mouse CCL22/MDC Quantikine ELISA Kit (MCC220) from R&D Systems.

Cell culture

786-O, RENCA and B16F0 cells were either a kind gift from the laboratory of Dr Serafim Kiriakidis, or from ATCC. Cells were incubated at 37°C in humidified air with 5% CO_2.

786-O cells were cultured in RPMI culture media containing 10% foetal bovine serum (FBS), 1% penicillin/streptomycin (p/s) and 1% glutamine. RENCA culture medium was further supplemented with 1% glutamine and 1 mM sodium pyruvate. Renal cancer cell lines were luciferase labelled for *in vivo* experiments. B16F0 were cultured in Dulbecco's Modified Eagle Medium (DMEM) containing 10% FBS and 1% p/s.

Migration assays

Chemotaxis was assayed using the Falcon PET Cell Culture Inserts, 8 μm pore (353182, Becton Dickinson, Franklin Lanes, NJ). 786-O cells were seeded in the upper chamber at $1x10^5$ in 0.5 ml serum-free RPMI and 1 ml of medium alone or supplemented with recombinant chemokines was added to the lower chamber. RENCA cells were seeded at $2x10^5$ in medium containing 1% serum. After overnight incubation at 37°C and 5% CO_2 cells on the upper surface of the filter were removed and migrated cells on the lower surface were stained with DiffQuik (Dade Behring, Deerfield, IL). For each insert, the number of migrated cells/field (40x for 786-O, 20x for RENCA) was counted. The assays were performed in triplicate.

Anti-CCR4 antibody

Affi-5 is a human IgG1 antibody antagonist of CCR4. This antibody is also referred to as 503 (18). It was produced by transient transfection of expression vectors into HEK-293T cells with FuGENE transfection reagent (Promega, Madison, WI). The ADCC enhanced (defucosylated) variant was produced using a selective class I a-mannosidase inhibitor, kifunensine (Sigma-Aldrich) that was added to the culture medium at a concentration of 100ng/ml. The antibody was then purified using standard conditions and formulated in

20mM Phosphate buffered saline 145mM NaCl pH7.2. It was diluted to the required concentration in the same buffer.

In vivo experiments

For the renal model, 6-8 week old female Balb/c or Balb/c *nu/nu* mice from Charles River (UK) were injected orthotopically with $1x10^5$ luciferase-labelled RENCA cells resuspended in Matrigel (354248, BD Biosciences, Becton Dickinson, Franklin Lanes, NJ) into the kidney capsule of the left kidney. Affi-5 and the appropriate isotype control where injected intra-peritoneally twice weekly at 10 or 20 mg/kg, starting at day 2 after surgery.

Tumor weight was determined at the end of the experiment by subtracting the right kidney weight from the weight of the tumor-bearing left kidney.

Tumor growth was monitored after administration of luciferin (3 mg/mouse, Sigma-Aldrich) with the IVIS Imaging System 100 (Xenogen Biosciences, Cranbury, NJ). Mice were sacrificed between day 17 and day 12 post-surgery.

The anti-MHCII blocking antibody (clone M5/114) and the isotype control (LTF-2) were obtained from BioXCell (West Lebanon, NH) and administered i.p. at 10 mg/kg one day prior to surgery and three times/week thereafter.

For the melanoma model, 8-12 week old C57/BL6 mice from Charles River (UK) were injected subcutaneously with $1x10^5$ B16F0 cells resuspended in PBS. Affi-5 and the appropriate isotype control where injected intra-peritoneally twice weekly at 20 mg/kg, starting at day 2 after surgery. Mice were sacrificed at day 18 post-injection.

Flow cytometry and sorting

Human cell lines were dissociated using cell dissociation buffer (Invitrogen) and stained with anti-CCR4 (R&D systems, FAB1567P) or IgG2B isotype control (R&D Systems). After washing, cells were incubated with Alexa-594 anti-mouse antibody (Invitrogen, Carlsbad, CA). Intracellular staining was achieved using saponin permeabilisation before antibodies against CCL17 and CCL22 were applied (R&D Systems, IC364IP and IC3361P respectively). RENCA murine cells were stained with Affi-5 or isotype control. After washing, cells were incubated with Alexa488 anti-human antibody (Invitrogen). Tumor-bearing left kidneys were chopped and incubated in 2 mg/ml collagenase V (Sigma-Aldrich), and 25 µg/ml DNAse (Roche, Basel, Switzerland), in HBSS (Sigma-Aldrich) for 45 min at 37˚C, 5% CO_2. Tumor-bearing kidneys were selected to be representative of the average tumor weight of the treatment group they belonged to. The lysate was strained with 70 µm strainers (Fisher Scientific, Loughborough, UK), and red blood cells were lysed (BD Pharm Lyse, BD Bioscience). Cells were counted and $6x10^6$ cells were stained in PBS + 2% heat inactivated FBS + 2 mM EDTA after blocking with αCD16/CD32 (14-0161, eBioscience, San Diego, CA) for 15 min. Staining antibodies were diluted 1:200 unless differently specified: αCD45 (48-0451, eBioscience), αFoxP3 (56-5773, eBioscience), αCD3 (45-0031, eBioscience), αCD4 (560783, BD Bioscience, 1:300), αCD8 (48-0041, eBioscience, 1:300), αLy-6C (45-5932, eBioscience), αLy-6G (Gr-1) (35-5931, eBioscience), αCD49b (108918, BioLegend, San Diego, CA), αF4/80 (47-4801, eBioscience, 1:150), αCD11b (11-0112, eBioscience), αMMR (141706, BioLegend), αMHCII (17-5321, eBioscience), αCCR4 (131214, BioLegend), αCD4 (560783, BD Biosciences, 1:300), αKi67 (612472, BD Biosciences, 5 µl/staining). Appropriate isotype

control antibodies were used to generate Fluorescence Minus One controls. Viability was assessed with Fixable Viability Dye eFluor780 or 506 (eBioscience) diluted 1:1000. Staining was performed for 30 min at 4˚C. Cells were washed, fixed in 2% formaldeyde, and analysed using a BD LSR Fortessa cytometer. Analysis was performed with the FlowJo software (Ashland, OR).

For the sorting of TAMs, tumors were dissected and dissociated as described above. Cells were stained in PBS + 2% heat inactivated FBS + 2 mM EDTA after blocking with αCD16/CD32 (14-0161, eBioscience) for 15 min. Staining antibodies were from eBioscience and were diluted 1:200 unless differently specified: αCD45 (48-0451), αLy6G (Gr-1) (35-5931), αF4/80 (47-4801, 1:150) αCD11b (11-0112), for 30 min at 4˚C. DAPI (2.5 µg/ml) was added prior to sorting, which was performed with a BD FACSARIA II cell sorter.

Suppression assay

Tumors were dissociated as for flow cytometry staining and pooled. MDSCs were purified according to manufacture's instructions using the Myeloid-Derived Suppressor Cell Isolation kit (Miltenyi Biotech, Bergish Gladbach, Germany). Naïve CD3 were isolated from spleen of healthy mice using the Dynabeads FlowComp Pan T kit (Invitrogen). Before stimulation, CD3 cells were prelabelled with 5 µM CSFE (eBioscience) for 5 min at 37˚C in medium and washed. Part of the cells was left without stimulus, while the remaining was stimulated with anti-CD3 anti CD28 coated beads (Dynabeads Mouse T-Activator CD3/CD28, Invitrogen) at a ratio 1:2 (beads:CD3) and plated ($5x10^4$/well) in round-bottom 96-wells. MDSCs were added to the wells at a

ratio of 10:1, 1:1, 1:2, 1:8 (CD3:MDSCs) and incubated for three days. At the end of the incubation period, cells were collected and stained for viability, CD11b, CD3, CD4 and CD8 for flow cytometry. Staining was performed for 30 min at 4˚C. Cells were washed, fixed in 2% formaldeyde, and analysed using a BD LSR Fortessa cytometer. Analysis was performed with the FlowJo software. CD4 or CD8 cells that had undergone at least one cycle of cell division were gated as proliferating.

Intracellular flow cytometry

Tumors were dissected and dissociated as described above. For macrophage staining, cells were plated (0.5x106/500 µl in a 24 well-plate) and incubated overnight with Brefeldin A (Sigma-Aldrich) 20 µg/ml. The following day, cells were stained in PBS + 2% heat inactivated FBS + 2 mM EDTA after blocking with αCD16/CD32 1:200 (14-0161, eBioscience) for 15 min. Staining antibodies were from eBioscience and were diluted 1:200 unless differently specified: αCD45 (48-0451), αLy-6G (Gr-1) (35-5931), αF4/80 (47-4801, 1:150) αCD11b (11-0112), and Fixable Viability Dye eFluor780 or 506 (eBioscience) diluted 1:1000 for 30 min at 4˚C. After washing, cells were fixed in Intracellular Fixation Buffer (eBioscience) for 20 min at RT. Cells were further permeabilized and stained in Permeabilization buffer with αTNF (11-7321-81, eBioscience) 1:75 in 25 µl, or the appropriate isotype control, for 30 min at 4˚C. After washing, cells were analysed using a BD LSR Fortessa cytometer. Analysis was performed with the FlowJo software. For CD4/CD8 staining, lymphocytes were purified using Dynabeads FlowComp Mouse Pan T (Invitrogen) according to instructions, plated in 500 µl in a 24-well plate, incubated with PMA (50 ng/ml, Sigma-Aldrich) and

ionomycin (1 μg/ml, Sigma-Aldrich) for 1 hour, and further incubated in the presence of Brefeldin A (20 μg/ml, Sigma-Aldrich) for 3 hours. At the end of the incubation, cells were washed, blocked as above, and stained with αCD3 (45-0031, 1:200), αCD8 (48-0041, 1:300), αCD4 (47-0041, 1:200), from eBioscience, and Fixable Viability Dye eFluor506 1:1000, fixed in 2% formalin, and stored overnight at 4˚C. The day after, cells were permeabilized and stained with αIFNγ (17-7311, 1:100) and αTNF (11-7321-81, 1:75), or the appropriate isotype controls, from eBioscience in 25 μl in Permeabilization buffer for 30 min at 4˚C, and further processed and analyzed as specified above.

Cytokine expression

Frozen tumors were lysed with a GentleMACS M tube (Miltenyi) in PBS with Complete Protease Inhibitors (Roche). Triton-X 100 was added (1%), lysates were cleared by centrifugation and applied to ProteomeProfiler Mouse Cytokine Array Panel A membranes (R&D System). An equivalent amount of 200 μg tumor lysate was incubated according to manufacturer's instructions. Film exposures were quantified using ImageJ software subtracting a lane background.

In vitro Th1 polarization assay.

Splenocytes from healthy Balb/c mice were obtained by mashing spleens through a 70 μm strainer and lysis of red blood cells. CD4+ cells were purified with the Miltenyi CD4+ T cell purification kit according to manufacturer's instructions. CD4+ cells were resuspended in IMDMEM 10%FBS, 50 μM b-mercaptoethanol, glutammine 8 mM, and stimulated with beads 1:1 Dynabeads® Mouse T-Activator CD3/CD28 (Invitrogen), mouse IL-2 20 ng/ml and mouse IL-12 5 ng/ml (from RnD System). The day after, the

indicated concentrations of CCL17 or CCL22 in combination with Affi-5 (30 µg/ml) were added to the plate. Experiments with Affi-5 were performed in Corning Ultra-low attachment plasticware (Cornig Life Sciences, Cornig, NY). Cells were stimulated with Restimulation cocktail plus transport inhibitor from ebioscience for 5 hours, and stained for 30 min at 4˚C with αCD16/CD32 (14-0161, eBioscience, 1:200), Fixable Viability Dye efluor450 1:1000, αCD4 (560783, BD Horizon CD4, BD Bioscience, 1:300) in 50 µl FACS buffer. After washing, cells were permeabilized and stained with αIFNγ (17-7311, eBioscience, 1:100), or isotype control. After washing, cells were analysed using a BD LSR Fortessa cytometer.

Immunofluorescence

Renal carcinoma 786-O and RENCA cells were cultivated on a chamber slide (Nalge Nunc International, Penfield, NY) for 1-2 days. Cells were then fixed for 30 min with 4% formaldehyde and permeabalised with 0.5% Triton X-100 in PBS for 10 min. Samples blocked with 1% BSA for 2 hours at RT, then incubated overnight at 4˚C with 25 mg/ml of α-CCR4 (IMG-322, IMGENEX, Novus Biologicals, Litteton, CO). After washing, samples were incubated with Alexa-594 secondary antibody, 1:2000 for 2 hours at RT. Finally, samples were washed mounted with Prolong Gold DAPI (Invitrogen, P36931). Cells were then visualized using a Zeiss LSM510 confocal microscope (Zeiss, Oberkochen, Germany).

RNA interference for CCR4 in renal cancer cell lines

Commercially available shRNAs, based on the pRS vector, were purchased from Origene Technologies (Rockville, MD). Four non-overlapping sequences were provided to target

human (TR314127) and mouse (TR500386) CCR4. A non-specific shRNA sequence (shGFP, TR30003) and empty pRS vector (TR20003) served as controls. Phoenix packaging cell line was transfected overnight with LipofectAMINE 2000 (Invitrogen) and 5 µg of the shRNA plasmid DNA. After an incubation with complete medium at 33°C and 5% CO_2 for 16 hours, the supernatant was collected, filtered, diluted 8:10 in RCC medium with the addition of polybrene. RENCA or 786-O at 30% confluence were infected for 10 h twice within 48 h. Virus-infected cells were selected with 1.5 µg/ml puromycin (InvivoGen). For long-term silencing in vivo, RENCA-luc cells were infected with three lentiviral GIPZ vectors targeting mouse CCR4 from Thermo Fisher Scientific (Waltham, MA). Viral particles were obtained by transfecting HEK293T with Ca-Phosphate method with 21 µg shRNA construct, 7 µg VSVG construct, 14 µg HIV construct (from Addgene, Cambridge, MA), in a 14-cm dish, and collecting the supernatant for 24 h. RENCA-luc were infected for 24 h in a 6-well plate with 1 ml supernatant. Virus-infected cells were selected with 0.3 µg/ml puromycin (Sigma). After verifying the silencing, cells infected with vector V3LMM_439088 were chosen for the in vivo experiment.

Statistical analysis

All data are expressed as the mean ± the standard error (SE) of the mean. Differences were considered significant at $p < 0.05$, using a Student's T-Test (two-tailed), ANOVA test or non-parametric test as appropriate, performed with the statistical analysis software Prism. P values are specified.

Study approval

Patients samples were collected under the Ethical Number MREC 02/8/78.

All experimental procedures observed the guidelines approved by the ethics committees of QMUL under the Home Office licence 70/7411.

Acknowledgements

The study was supported by CRUK programme grant C587/A16354 and a research grant from Affitech AS. We would like to thank Prof. Yaohe Wang (Barts Cancer Institute, London) for his help in setting up CCR4, CCL17 and CCL22 immunohistochemistry staining, Dr. David Gould (William Harvey Research Institute, London) for luciferase-labeling our renal cancer cell lines, Dr. Melania Capasso and Mark Brown (Barts Cancer Institute, London) for assistance with the silencing experiments, Dr. Alzbeta Talarovicova (Barts Cancer Institute, London) for assistance with the mouse work, and Dr. Matthew McCourt (Actigen, Cambridge) for helpful discussion.

Author Contributions

CB designed, performed, and interpreted most of the experiments, and wrote the manuscript. MNK designed, performed, and interpreted the experiments shown in Fig. 1 and Suppl. Fig. 1-3. TS, AM and EM contributed designing, performing, and interpreting some experiments and editing the manuscript. RT performed most of the surgery experiments. MJ conducted and analyzed the B16 melanoma studies. MC measured and analyzed the chemokine levels in patients. HK contributed to design of the research studies. UBH and AD provided the Affi-5 antibody and contributed to the design of the experiments. LF and RWW contributed to the design of the research studies and editing the manuscript. TP provided patient samples, patient information and intellectual input, SQ contributed designing and interpreting crucial experiments analysing adaptive immunity. FB conceived of, designed, and supervised the project and experimental plan, interpreted experiments, and wrote the manuscript.

References

1. Raman D, Sobolik-Delmaire T, and Richmond A. Chemokines in health and disease. *Exp Cell Res.* 2011;317(5):575-89.
2. Allavena P, Germano G, Marchesi F, and Mantovani A. Chemokines in cancer related inflammation. *Exp Cell Res.* 2011;317(5):664-73.
3. Mantovani A, Savino B, Locati M, Zammataro L, Allavena P, and Bonecchi R. The chemokine system in cancer biology and therapy. *Cytokine Growth Factor Rev.* 2010;21(1):27-39.
4. Zlotnik A, Burkhardt AM, and Homey B. Homeostatic chemokine receptors and organ-specific metastasis. *Nat Rev Immunol.* 2011;11(9):597-606.
5. Balkwill FR. The chemokine system and cancer. *The Journal of pathology.* 2012;226(2):148-57.
6. Bonecchi R, Bianchi G, Bordignon PP, D'Ambrosio D, Lang R, Borsatti A, Sozzani S, Allavena P, Gray PA, Mantovani A, et al. Differential expression of chemokine receptors and chemotactic responsiveness of type 1 T helper cells (Th1s) and Th2s. *J Exp Med.* 1998;187(1):129-34.
7. Kunkel EJ, Boisvert J, Murphy K, Vierra MA, Genovese MC, Wardlaw AJ, Greenberg HB, Hodge MR, Wu L, Butcher EC, et al. Expression of the chemokine receptors CCR4, CCR5, and CXCR3 by human tissue-infiltrating lymphocytes. *Am J Pathol.* 2002;160(347-55.
8. Imai T, Nagira M, Takagi S, Kakizaki M, Nishimura M, Wang J, Gray PW, Matsushima K, and Yoshie O. Selective recruitment of CCR4-bearing Th2 cells toward antigen-presenting cells by the CC chemokines thymus and activation-regulated chemokine and macrophage-derived chemokine. *International immunology.* 1999;11(1):81-8.
9. Yoshie O, and Matsushima K. CCR4 and its ligands: from bench to bedside. *International immunology.* 2015;27(1):11-20.
10. Curiel TJ, Coukos G, Zou L, Alvarez X, Cheng P, Mottram P, Evdemon-Hogan M, Conejo-Garcia JR, Zhang L, Burow M, et al. Specific recruitment of regulatory T cells in ovarian carcinoma fosters immune privilege and predicts reduced survival. *Nature medicine.* 2004;10(9):942-9.
11. Jacobs JF, Idema AJ, Bol KF, Grotenhuis JA, de Vries IJ, Wesseling P, and Adema GJ. Prognostic significance and mechanism of Treg infiltration in human brain tumors. *J Neuroimmunol.* 2010;225(1-2):195-9.
12. Yang P, Li QJ, Feng Y, Zhang Y, Markowitz GJ, Ning S, Deng Y, Zhao J, Jiang S, Yuan Y, et al. TGF-beta-miR-34a-CCL22 signaling-induced Treg cell recruitment promotes venous metastases of HBV-positive hepatocellular carcinoma. *Cancer Cell.* 2012;22(3):291-303.
13. Gobert M, Treilleux I, Bendriss-Vermare N, Bachelot T, Goddard-Leon S, Arfi V, Biota C, Doffin AC, Durand I, Olive D, et al. Regulatory T Cells Recruited Through CCL22/CCR4 are Selectively Activated in Lymphoid Infiltrates Surrounding Primary Breast Tumors and Lead to an Adverse Clinical Outcome. *Cancer Res.* 2009;69(5):2000-9.

14. Li JY, Ou ZL, Yu SJ, Gu XL, Yang C, Chen AX, Di GH, Shen ZZ, and Shao ZM. The chemokine receptor CCR4 promotes tumor growth and lung metastasis in breast cancer. *Breast cancer research and treatment.* 2012;131(3):837-48.
15. Lee JH, Cho YS, Lee JY, Kook MC, Park JW, Nam BH, and Bae JM. The chemokine receptor CCR4 is expressed and associated with a poor prognosis in patients with gastric cancer. *Annals of surgery.* 2009;249(6):933-41.
16. Ishida T, Joh T, Uike N, Yamamoto K, Utsunomiya A, Yoshida S, Saburi Y, Miyamoto T, Takemoto S, Suzushima H, et al. Defucosylated anti-CCR4 monoclonal antibody (KW-0761) for relapsed adult T-cell leukemia-lymphoma: a multicenter phase II study. *J Clin Oncol.* 2012;30(8):837-42.
17. Ogura M, Ishida T, Hatake K, Taniwaki M, Ando K, Tobinai K, Fujimoto K, Yamamoto K, Miyamoto T, Uike N, et al. Multicenter phase II study of mogamulizumab (KW-0761), a defucosylated anti-cc chemokine receptor 4 antibody, in patients with relapsed peripheral T-cell lymphoma and cutaneous T-cell lymphoma. *J Clin Oncol.* 2014;32(11):1157-63.
18. Sugiyama D, Nishikawa H, Maeda Y, Nishioka M, Tanemura A, Katayama I, Ezoe S, Kanakura Y, Sato E, Fukumori Y, et al. Anti-CCR4 mAb selectively depletes effector-type FoxP3+CD4+ regulatory T cells, evoking antitumor immune responses in humans. *Proc Natl Acad Sci U S A.* 2013;110(44):17945-50.
19. Hagemann UB, Gunnarsson L, Geraudie S, Scheffler U, Griep RA, Reiersen H, Duncan AR, and Kiprijanov SM. Fully human antagonistic antibodies against CCR4 potently inhibit cell signaling and chemotaxis. *PLoS One.* 2014;9(7):e103776.
20. Sica A, Larghi P, Mancino A, Rubino L, Porta C, Totaro MG, Rimoldi M, Biswas SK, Allavena P, and Mantovani A. Macrophage polarization in tumour progression. *Semin Cancer Biol.* 2008;18(5):349-55.
21. Porta C, Rimoldi M, Raes G, Brys L, Ghezzi P, Di Liberto D, Dieli F, Ghisletti S, Natoli G, De Baetselier P, et al. Tolerance and M2 (alternative) macrophage polarization are related processes orchestrated by p50 nuclear factor kappaB. *Proc Natl Acad Sci U S A.* 2009;106(35):14978-83.
22. Overdijk MB, Verploegen S, Ortiz Buijsse A, Vink T, Leusen JH, Bleeker WK, and Parren PW. Crosstalk between human IgG isotypes and murine effector cells. *J Immunol.* 2012;189(7):3430-8.
23. Liu Q, Rexiati M, Yang Y, Wang WG, Azhati B, Saimaiti W, and Wang YJ. Expression of chemokine receptor 4 was associated with poor survival in renal cell carcinoma. *Medical oncology.* 2014;31(4):882.
24. Pyonteck SM, Akkari L, Schuhmacher AJ, Bowman RL, Sevenich L, Quail DF, Olson OC, Quick ML, Huse JT, Teijeiro V, et al. CSF-1R inhibition alters macrophage polarization and blocks glioma progression. *Nat Med.* 2013;19(10):1264-72.
25. Dannenmann SR, Thielicke J, Stockli M, Matter C, von Boehmer L, Cecconi V, Hermanns T, Hefermehl L, Schraml P, Moch H, et al. Tumor-associated macrophages subvert T-cell function and correlate with reduced survival in clear cell renal cell carcinoma. *Oncoimmunology.* 2013;2(3):e23562.
26. Beck A, and Reichert JM. Marketing approval of mogamulizumab: a triumph for glyco-engineering. *mAbs.* 2012;4(4):419-25.

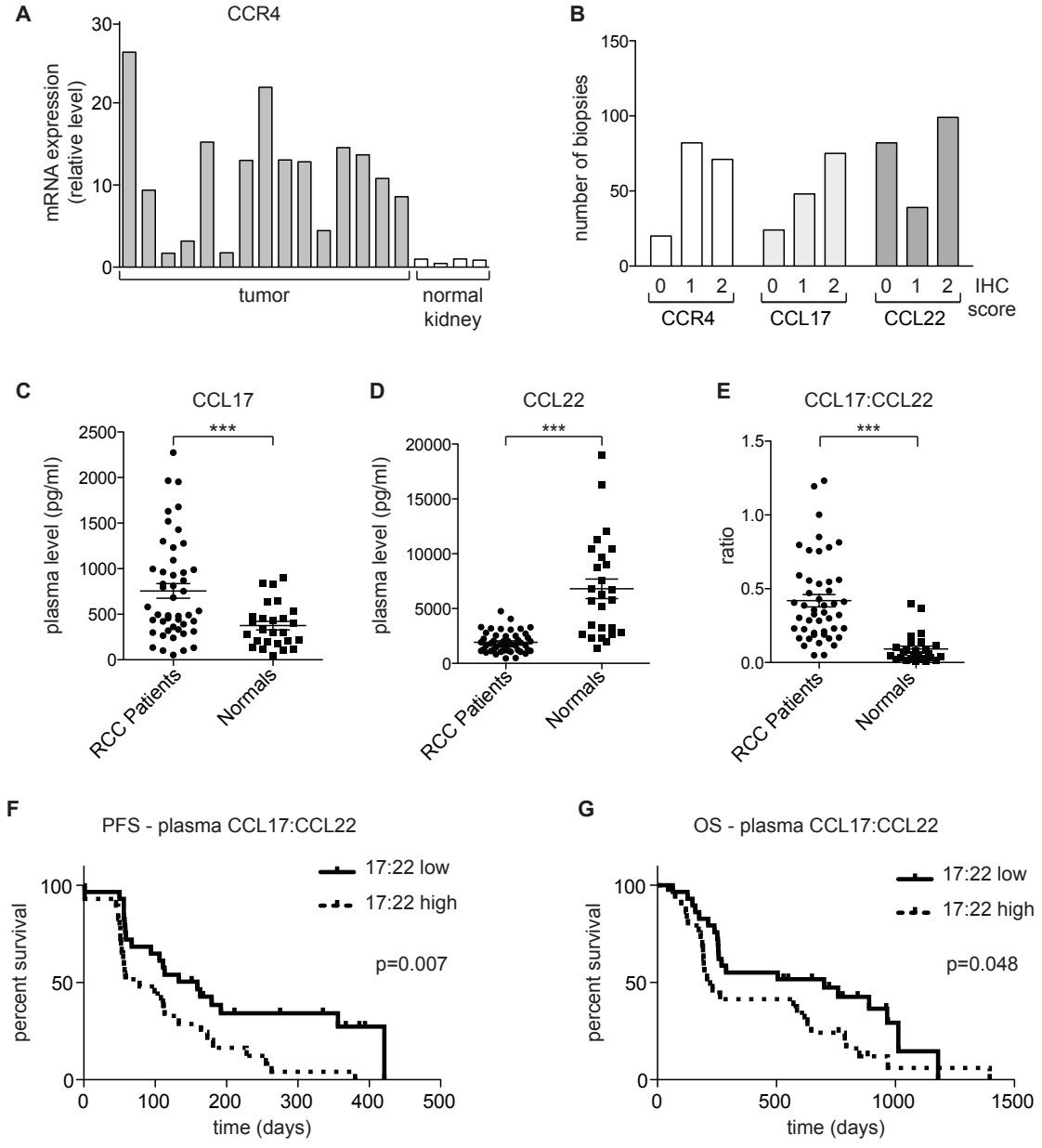

Figure 1

Figure 1

Abnormal expression of CCR4 and its ligands in human renal cancer. (**A**) CCR4 mRNA was measured by real-time RT-PCR in renal cell cancer, RCC, biopsies and compared with normal kidney. (**B**) Levels of CCR4 and its ligands CCL17 and CCL22 were analysed by IHC

in a tissue microarray (TMA) of renal cancer biopsies from human patients. Each biopsy was scored 0 – no staining, 1 – weak staining, 2 – strong staining for CCR4, CCL17 and CCL22. A total of 173 biopsy cores from 57 patients were stained for CCR4 and CCL22, and 145 cores from 48 patients for CCL17. (**C, D, E**) Plasma levels of CCL17, CCL22 and the CCL17:22 ratio in RCC patient plasma were compared to normal individuals of matched age using Mesoscale Discovery System Ultra-Sensitive plates. (n=47 for RCC patients, n=26 for normals, two-tailed Student's *t* test, ***p= 0.0001 for CCL17, ***p<0.0001 for CCL22, ***p< 0.0001 for CCL17:CCL22). (**F**, **G**) Kaplan-Meier survival curves for progression free survival (**F**) and overall survival (**G**) for RCC patients with CCL17:CCL22 high (above the median) or low (n=57). For progression free survival, hazard ratio 0.436, 95% CI 0.239 to 0.797, for overall survival, hazard ratio 0.552, 95% CI 0.306 to 0.995.

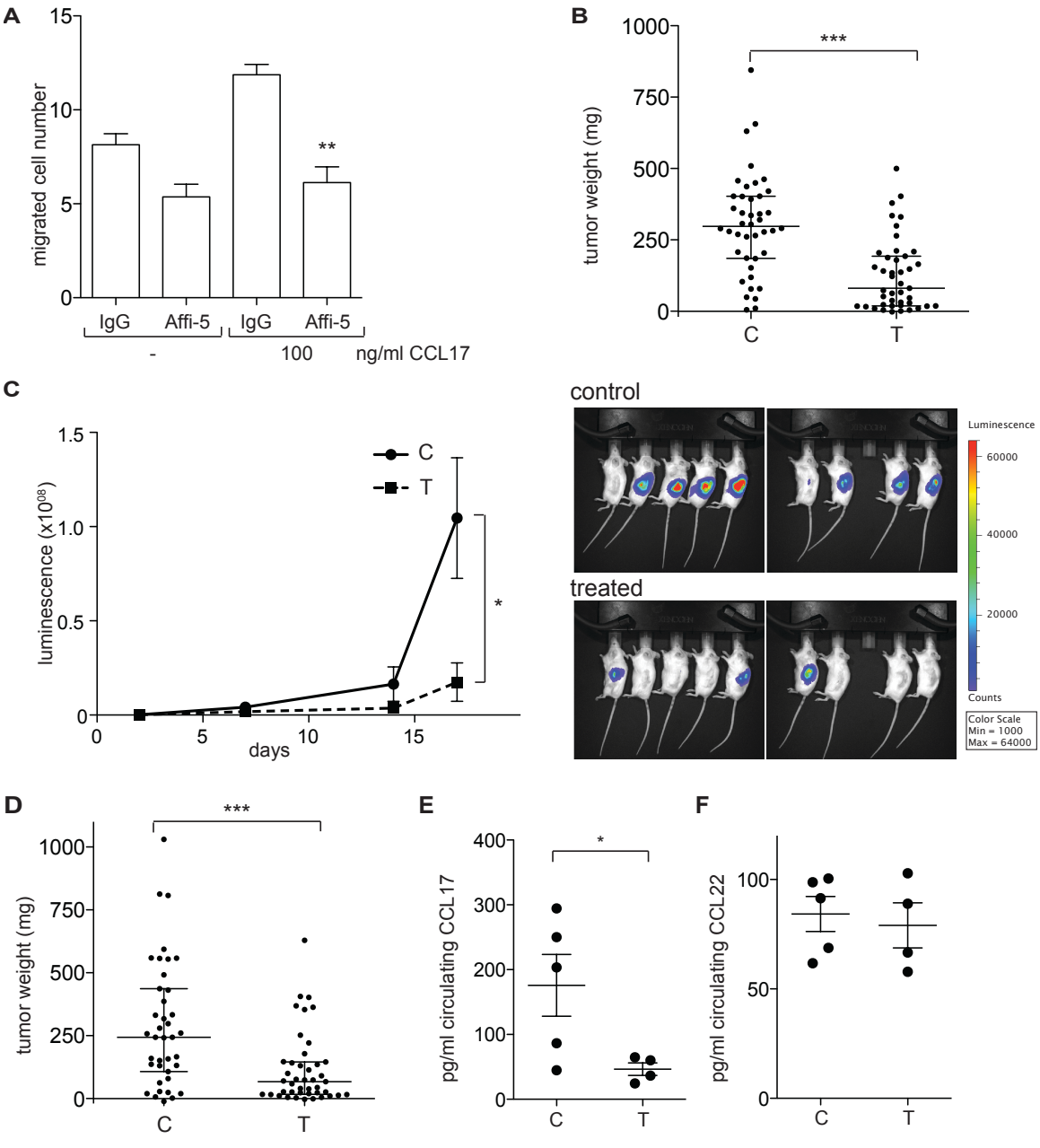

Figure 2

Figure 2

Anti-CCR4 antibody Affi-5 has anti-tumor activity in the RENCA RCC model. (**A**) Migration of RENCA cells in response to mouse CCL17 in the presence of 10 µg/ml Affi-5 or isotype control IgG after an incubation of 16 hours was analysed with a migration assay. Significant difference compared to the CCL17-induced migration in the presence of

isotype control is indicated, two-tailed Student's *t* test, ** p<0.01. CCL17-induced migration is significant compared to control (p<0.05). One experiment representative of three is shown. (**B**, **C**) Balb/c mice were injected with $1x10^5$ RENCA-luc cells and treated twice weekly with Affi-5 (T) or isotype control (C) at 20 mg/kg starting 48h after surgery. Mice were sacrificed 17 days after surgery and tumor weight was determined. Combined results of six experiments are shown (n= 42 C, n= 43 T, two-tailed Student's *t* test, p<0.0001). Chemiluminescence was determined at day 7, 14, and 17 and one representative experiment is reported in the graph and pictures as relative luminescence units (**C**) two-tailed Student's *t* test, * p=0.029 at day 17. (**D**) Balb/c mice were injected with $1x10^5$ RENCA-luc cells and treated twice weekly with Affi-5 (T) or isotype control (C) at 10 mg/kg starting 48h after surgery. Mice were sacrificed 17 days after surgery and tumor weight was determined. Combined results of six experiments are shown (n= 39 C, n= 43 T, two-tailed Student's *t* test, p<0.0001). (**E**, **F**) Serum collected at end-point was analysed by ELISA for CCL17 and CCL22. Two-tailed Student's *t* test, * p=0.05, n=5 for samples from control treated (C) mice, n=4 for samples from Affi-5 treated (T) mice.

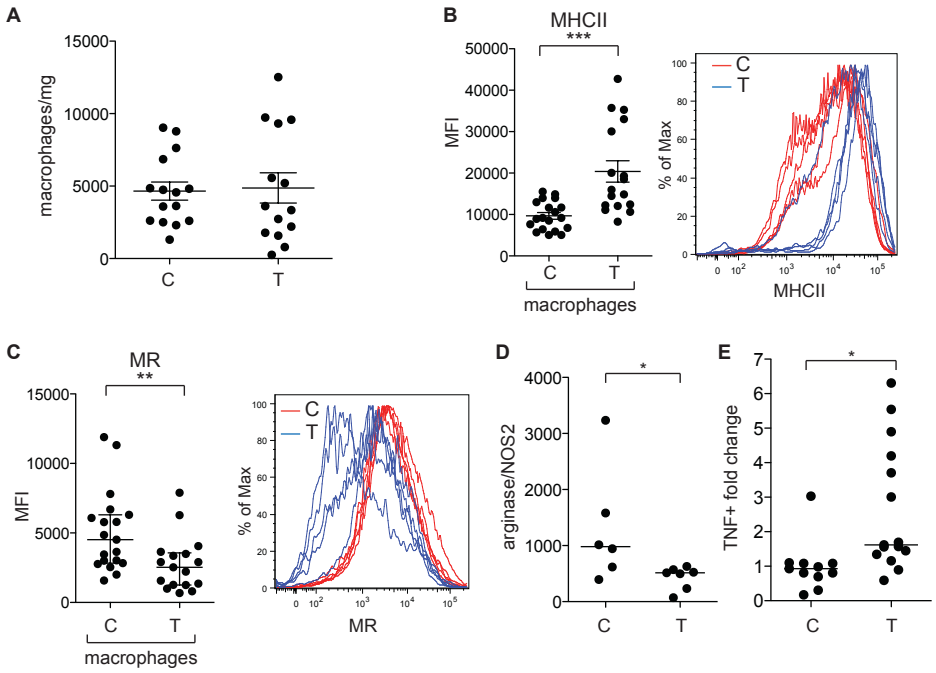

Figure 3

Figure 3

Effects of anti-CCR4 on the RENCA tumor associated macrophages. Balb/c mice were injected with RENCA-luc cells and treated with Affi-5 (T) or isotype control (C). Mice were sacrificed 17 days after surgery and tumors were dissociated and characterised by flow cytometry. (**A**) Tumor infiltrating macrophages (gated as CD45+ CD11b+ F4/80+) per mg of tumor for five independent experiments are shown. There was no significant difference between Affi-5-treated (T) and isotype-treated (C) tumors (n=15 and 14, respectively). (**B**, **C**) Geometric mean of fluorescence intensity for MHCII and MR staining on macrophages for five independent experiments, and staining for isotype-treated and Affi-503-treated dissociated tumors for one representative experiment. Two-tailed Student's *t* test, p=0.0008 and p=0.0085, respectively. n=19 for C, n=17 for T (**D**) RNA was extracted from macrophages (CD45+ CD11b+ F4/80+) sorted by flow cytometry from dissociated tumors. The ratio between arginase and NOS2 expression

was determined by real time PCR in two independent experiments pooled together (Mann-Whitney U test, p=0.035), with n=6 for C, and n=7 for T. (**E**) Cells were dissociated at endpoint from dissected tumors from Balb/c mice treated with Affi-5 (T) or isotype control (C) and plated overnight in the presence of brefeldin A. The fold change in the number of macrophages (CD45+ CD11b+ F4/80+) positive for intracellular TNFα is shown from two pooled experiments (Mann-Whitney U test, p=0.002, n=11 and 15).

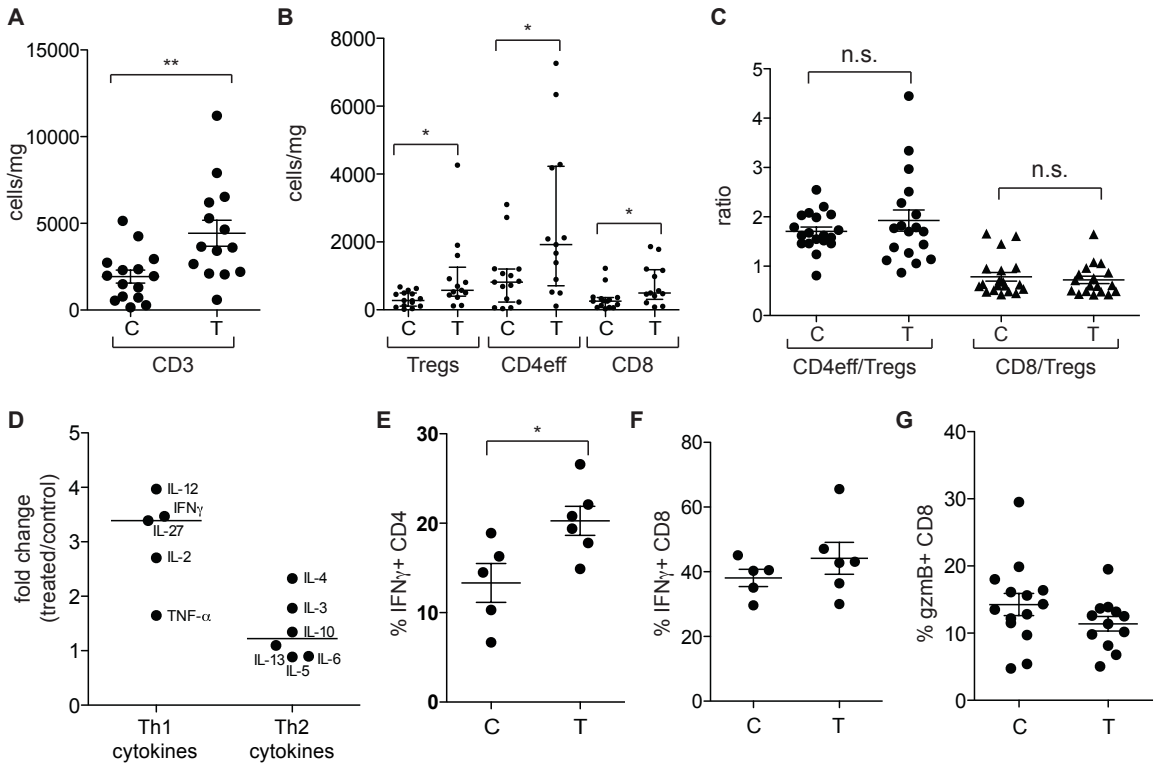

Figure 4

Figure 4

Involvement of T cells in the actions of the anti-CCR4 antibody. Balb/c mice were injected with RENCA-luc cells and treated with Affi-5 (T) or isotype control (C). Mice were sacrificed 17 days after surgery and tumors were dissociated and characterised by flow cytometry. (**A**, **B**) Number of CD45+CD3+ (A), CD4+ FoxP3+ (Tregs), CD4+ FoxP3- (CD4eff) and CD8+ cells/mg of tumor (B) in tumors from isotype-treated (C) or Affi-5-treated (T) mice for four experiments pooled together (two-tailed Student's *t* test, (A) p=0.003 and (B) p=0.01, p=0.02 and p=0.01 respectively, with n=15 for C, and 14 for T). (**C**) Ratio between CD3+, CD4+, FoxP3- or CD3+, CD8+ and CD3+, CD4+, FoxP3+ (Treg) lymphocytes in isotype-treated and Affi-5-treated mice for four experiments (**D**) Two

control-treated (control) and two Affi-5 treated (treated) tumors from Balb/c mice were lysed and an amount equivalent to 200 μg tumor lysate was incubated on Proteome Profiler Mouse Cytokine Array Panel A membranes. Average signal for each cytokine was normalised to signal from control-treated tumors. Fold change compared to control, grouped for Th1 cytokines and Th2 cytokines, is shown (two-tailed Student's *t* test, p= 0.0173). (**E, F**) CD3 cells were isolated at endpoint from dissected tumors from Balb/c mice treated with Affi-5 (T) or isotype control (C). Lymphocytes were stimulated with PMA and ionomycin for 4 hours in the presence of brefeldin A and stained for intracellular IFNγ. The percentage of IFNγ positive CD4+ cells (**E**) or CD8+ cells (**F**) is represented. Two independent experiments pooled together are shown (two-tailed Student's *t* test, p=0.028 for IFNγ positive CD4 cells, n=5 for C, n=6 for T). (**G**) Percentage of CD8 cells positive for granzyme B are represented, from four independent experiments.

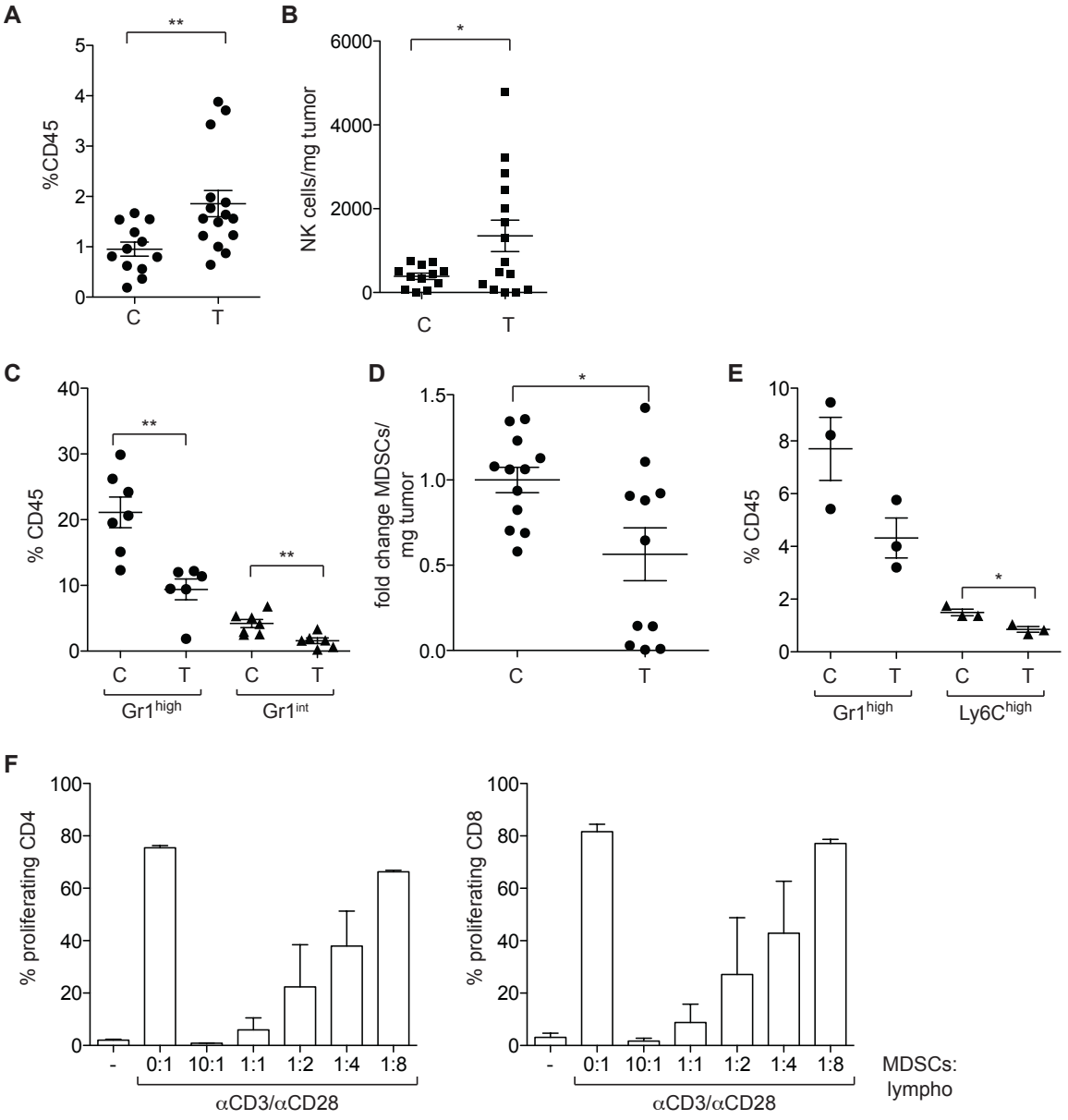

Figure 5

Figure 5

Other effects of anti-CCR4 antibody in the RENCA tumor model. Balb/c mice were injected with RENCA-luc cells and treated with Affi-5 (T) or isotype control (C). Mice were sacrificed 17 days after surgery and tumors or spleens were dissociated and characterised by flow cytometry. (**A**) Percentage of NK cells (CD45+ CD3- DX5+) among the CD45+ population in tumors, two-tailed Student's *t* test, p=0.0064, four

independent experiments pooled together (n=12 for C, n=15 for T). (**B**) The number of NK cells/mg of tumor was also significantly higher with treatment (two-tailed Student's *t* test, p=0.032, n=12 for C, n=15 for T). (**C**) Percentage of MDSCs (CD45+ CD11+ Gr1+) among the CD45+ infiltrate for tumors from control and treated animals. Two populations of MDSCs ($Gr1^{high}$ and $Gr1^{int}$) were identified and analysed separately. Two-tailed Student's *t* test, p=0.0021 and p=0.0065 for $Gr1^{high}$ and $Gr1^{int}$ respectively, two experiments pooled together, n=7 for C and n=6 for T. (**D**) The fold change of the number of MDSCs/mg of tumor was also significantly lower in the tumors from treated animals (four experiments, two-tailed Student's *t* test, p=0.017, n=12 for C, n=11 for T). (**E**) Percentage of MDSCs (CD45+ CD11b+ Gr1+) among the CD45+ infiltrate for spleens from control and treated animals. Two populations of MDSCs ($Gr1^{high}$ $Ly6C^{int}$ and $Ly6C^{high}$ $Gr1^{int}$) were identified and analysed separately. Two-tailed Student's *t* test, p=0.075 for $Gr1^{high}$, p=0.018 for $Ly6C^{high}$, n=3. (**F**) Naive CD3 isolated from spleen of healthy mice ($5x10^4$/well) were pre-labelled with CFSE and activated with anti-CD3 and anti-CD28-coated beads at a ratio 1:2 beads:CD3 cells in the presence of freshly isolated MDSCs from tumors. Cells were co-cultured for 3 days, and CD4+ and CD8+ T cell proliferation was measured by CFSE dye dilution from two independent experiments, each pooling MDSCs from two-three tumors. Proliferation was inhibited significantly (one-way ANOVA, p=0.0012 for CD4, p=0.0058 for CD8, at the MDSCs:T cells ratios of 10:1, 1:1, 1:2).

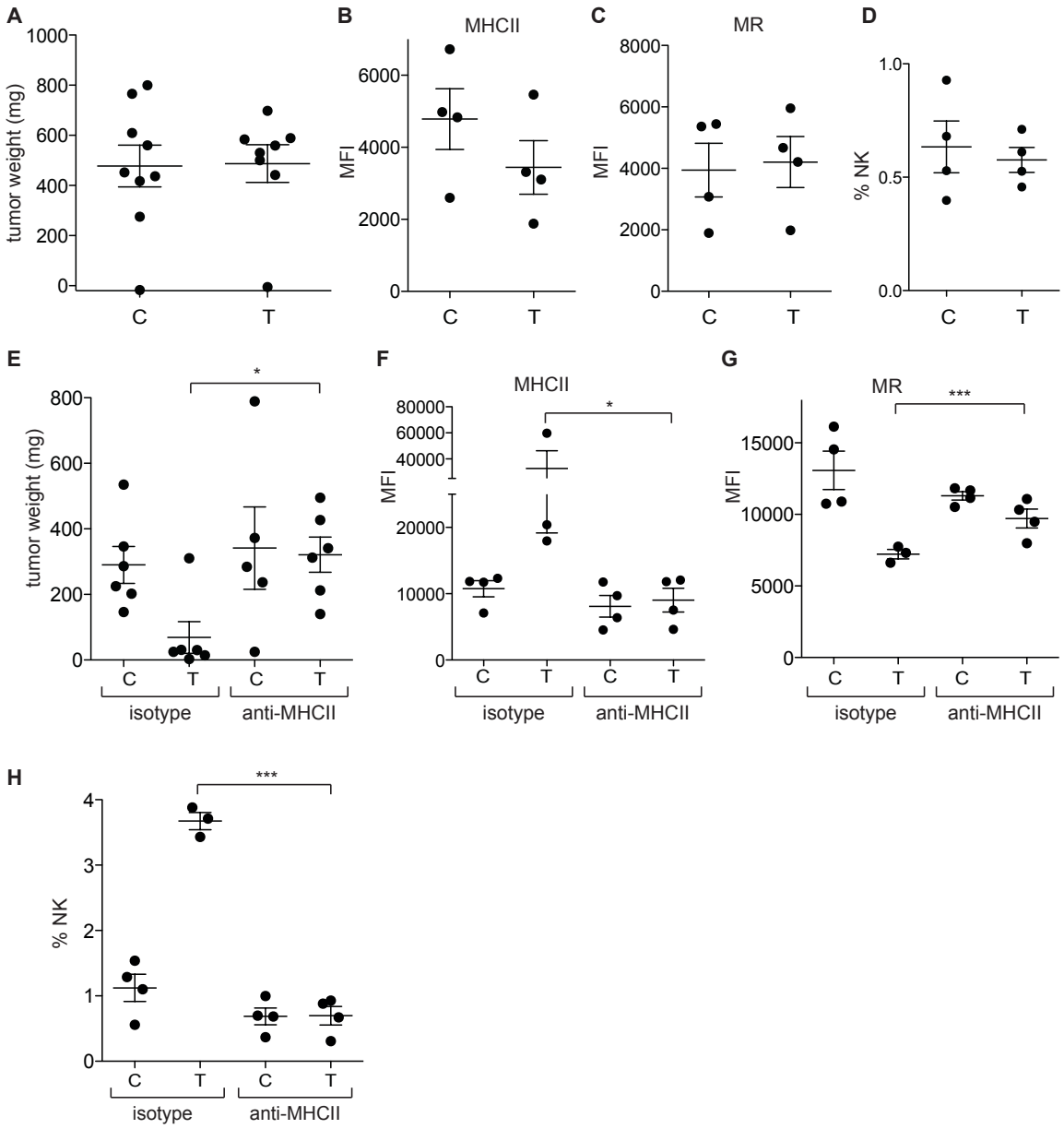

Figure 6

Figure 6

Effects of anti-CCR4 on the RENCA tumors require CD4 cells. (**A**, **B**, **C**, **D**) Balb/c *nu/nu* mice were injected with $1x10^5$ RENCA-luc cells and treated with Affi-5 (T) or isotype control (C) 10 mg/kg twice weekly starting 48h after surgery. Mice were sacrificed at 17 days after surgery and tumor weight was determined (n=9 C, n=8 T, non significant).

Geometric mean of fluorescence intensity for MHCII (**B**) and MR (**C**) staining on macrophages (CD45+, CD11b+ F4/80+), for isotype-treated and Affi-503-treated dissociated tumors, n=4. (**D**) Percentage of NK cells (CD45+ CD3- DX5+) among the CD45+ population, n=4. (**E**, **F, G**, **H**) Balb/c mice were injected with $1x10^5$ RENCA-luc cells and treated with Affi-5 (T) or isotype control (C) 10 mg/kg twice-weekly starting 48h after surgery. Treatment with anti-MHCII or the relevant isotype control (10 mg/kg) was started one day prior surgery and continued with three doses per week. Mice were sacrificed at 17 days after surgery and tumor weight was determined (n=6 for each group) and tumors were dissociated and characterised by flow cytometry. (**E**). Blocking of MHCII has a significant effect on tumor weight (two-way ANOVA, $p=0.049$). Bonferroni post test showed significant difference ($p<0.05$) between the weight of Affi-5 treated tumors in the presence or absence of anti-MHCII. (**F**, **G**) Geometric mean of fluorescence intensity for MHCII (F) and MR (G) staining on macrophages (CD45+, CD11b+ F4/80+). There is significant difference between MHCII and MR expression of macrophages from Affi-5 treated tumors in the presence or absence of anti-MHCII (two-tailed Student's *t* test, $p<0.05$ and $p<0.001$, respectively, with n=3-4 for each group) (**H**) Percentage of NK cells (CD45+ CD3- DX5+) among the CD45+ population. There is significant difference (two-tailed Student's *t* test, $p<0.001$) between the percentage of NK cells from Affi-5 treated tumors in the presence or absence of anti-MHCII.

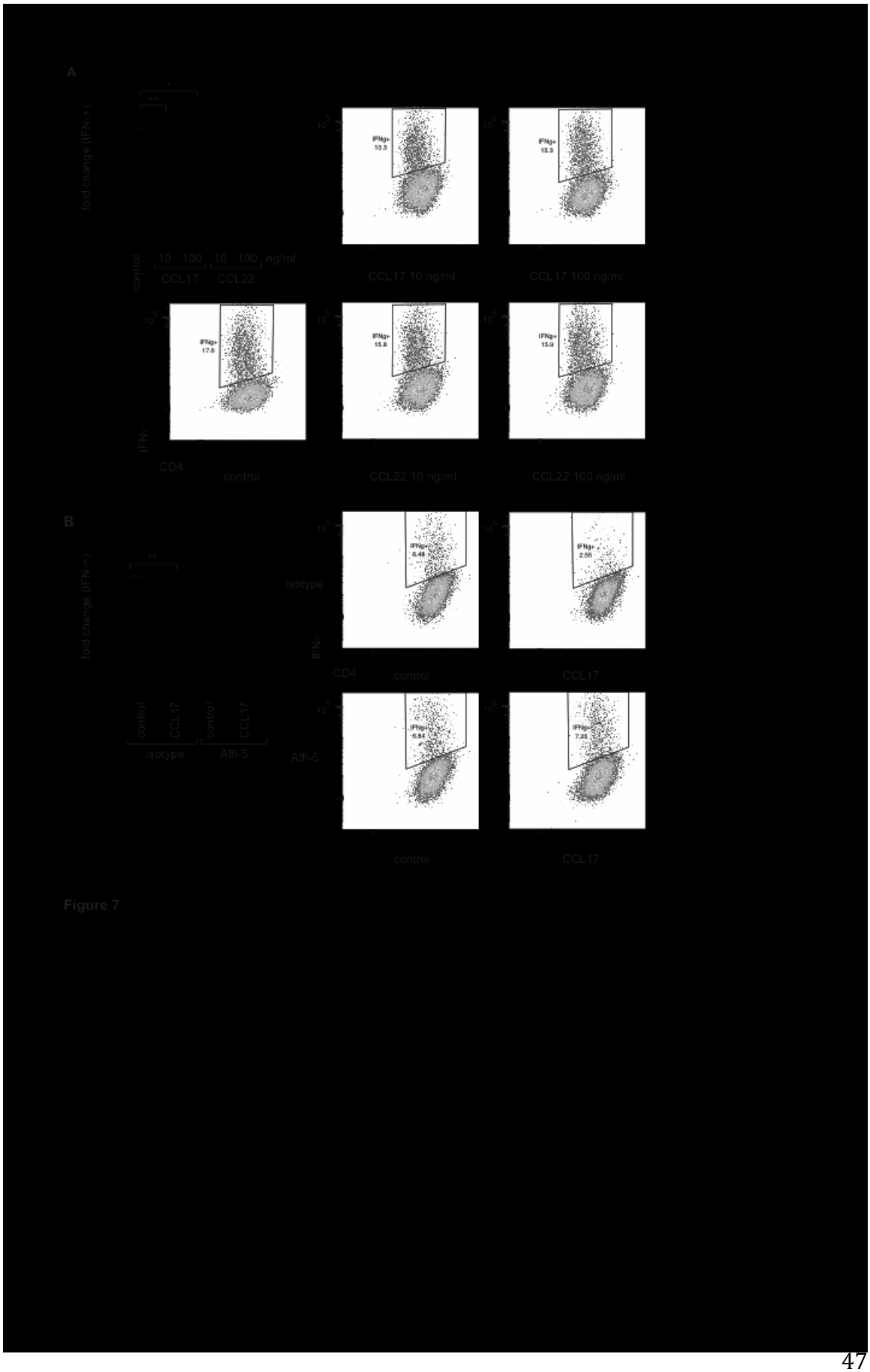
A
fold change (IFNg+)
control
10
100
10
100
ng/ml
CCL17
CCL22
IFNg+
13.3
IFNg+
15.3
IFNg+
17.0
IFNg+
15.8
IFNg+
15.9
IFNγ
CD4
control
CCL17 10 ng/ml
CCL17 100 ng/ml
CCL22 10 ng/ml
CCL22 100 ng/ml
B
fold change (IFNg+)
isotype
Affi-5
control
CCL17
control
CCL17
isotype
Affi-5
IFNg+
6.48
IFNg+
2.55
IFNg+
6.84
IFNg+
7.35
IFNγ
CD4
control
CCL17
control
CCL17

Figure 7

Figure 7

CCL17 can inhibit Th1 responses *in vitro.* (**A**, **B**) CD4+ cells were isolated from spleens of healthy mice and stimulated with IL-2 and IL-12 in the presence of ant-CD3 and anti-CD28 coated beads. CCL17, CCL22, Affi-5 (10 μg/ml) or isotype control were added after an overnight incubation, and after three days cells were stimulated with Cell stimulation cocktail, harvested and stained for intracellular IFNγ, and analysed by flow cytometry. Seven and three independent experiments are shown for CCL17 and CCL22, respectively (**A**), together with representative plots of one experiment. Four independent experiments are shown in (**B**), with representative plots for one experiment.

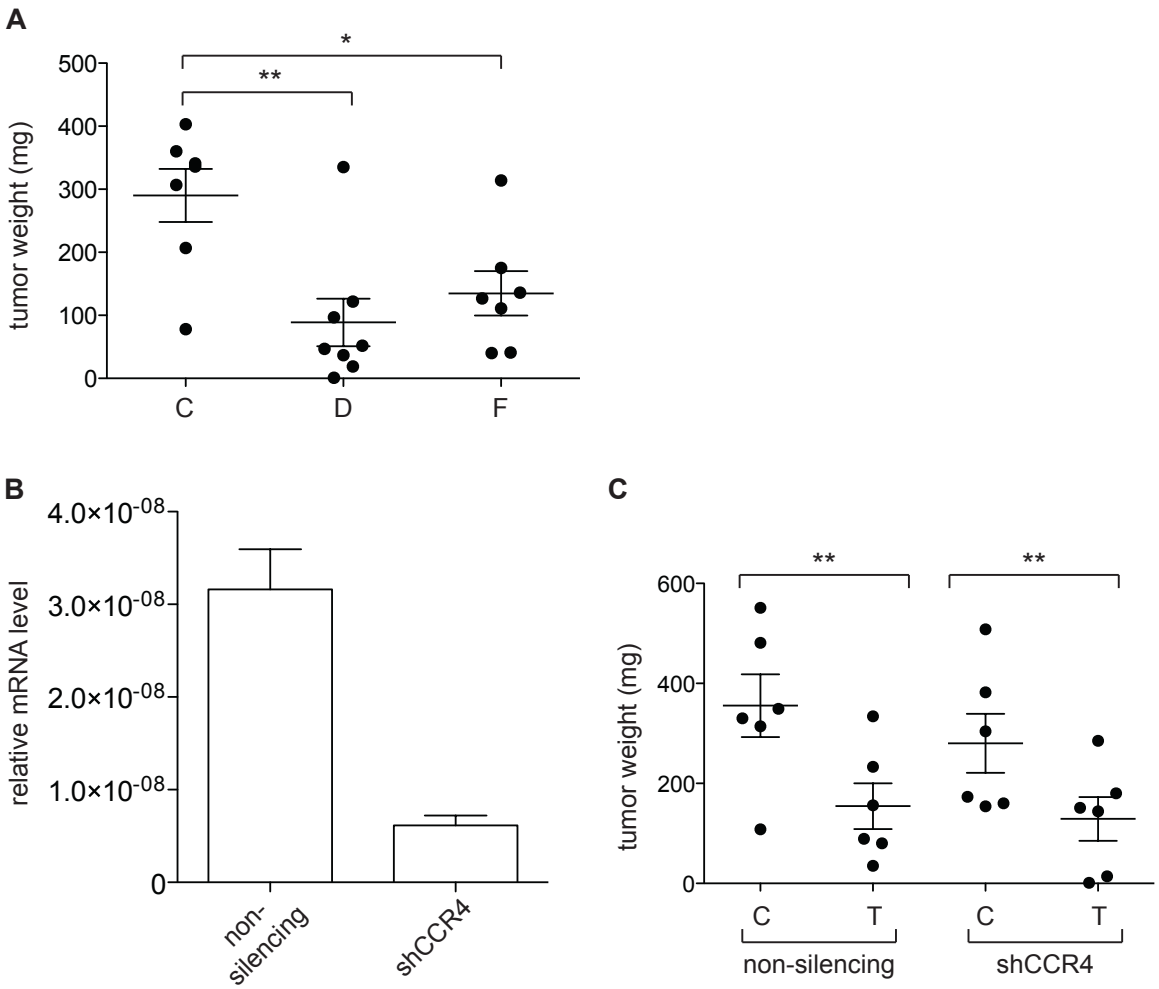

Figure 8

Figure 8

Effects of anti-CCR4 antibody is not dependent on malignant cell expression of CCR4. (**A**) Balb/c mice were injected with $1x10^5$ RENCA-luc cells and treated with defucosylated Affi-5 (T (D)), fucosylated Affi-5 (T (F)), or defucosylated isotype control (C) at 10 mg/kg twice weekly starting 48h after surgery. Mice were sacrificed 17 days after surgery and tumor weight was analysed (n=7 (C), n=8 T (D), n=7 T(F)). Two-tailed Student's *t* test, ** $p<0.01$, * $p<0.05$. (**B**) RENCA-luc cells were infected with lentivirus encoding for non-silencing shRNA, or anti-CCR4 shRNA. Silencing of the infected cells lines was verified at

the RNA level by RT-PCR. (C) Balb/c mice were injected with $1x10^5$ RENCA-luc cells infected with a non-silencing lentivirus, or CCR4 shRNA (shCCR4), and treated twice weekly with Affi-5 at 10 mg/kg (T) or isotype control (C), starting 48h after surgery, n=6 for each group. Mice were sacrificed 17 days after surgery and tumor weight was recorded. Affi-5 treatment had an effect (two-way ANOVA, p= 0.0036), and CCR4 silencing did not interact significantly with the Affi-5 treatment (p=0.64).